Positioning and Location-based Beamforming for High Speed Trains in 5G NR Networks

Jukka Talvitie*, Toni Levanen*, Mike Koivisto*, Tero Ihalainen†, Kari Pajukoski†,
Markku Renfors* and Mikko Valkama*
*Laboratory of Electronics and Communications Engineering, Tampere University of Technology, Finland
†Nokia Bell Labs, Finland
Email: jukka.talvitie@tut.fi

***Abstract*—High-accuracy positioning enables emerging of new vertical markets for the forthcoming fifth generation (5G) mobile networks. In this paper, we study network-side positioning and related location-based beamforming for high-speed train (HST) scenario in 5G New Radio (NR) networks. To avoid tight synchronization requirements between the train and the network, we consider Time-Difference-Of-Arrival (TDOA) measurements based on 5G NR uplink sounding reference signals. Moreover, in order to facilitate the location-based beamforming, we introduce methods for removing measurement outliers and for selecting the optimal reference measurement for the time-difference evaluations. The train is tracked by utilizing Extended Kalman Filter (EKF), which is capable to track and predict the train position for the location-based beamformer in real-time. Based on results obtained from extensive 5G NR compliant simulations, the proposed approach is able to achieve a sub-meter positioning accuracy with 90% availability, which is sufficient for many mission-critical positioning applications in the considered HST scenario.**

***Index Terms*—Positioning, Location-based beamforming, Fifth generation mobile networks, 5G, New Radio, NR, High-speed trains, HST**

I. Introduction

The high-speed train (HST) networks establish one of the most promising vertical markets emerging from the fifth generation (5G) new radio (NR) technologies. Compared to previous generation technologies, 5G NR introduces various new features, such as increased subcarrier spacing, new reference signals and reduced time slot durations, for improved system performance in the high-speed scenario. In addition, the 5G NR supports new millimeter wave bands enabling utilization of larger bandwidths with increased data throughput, and facilitating massive beamforming.

The considered baseline HST network structure and the related system parametrization has been specified by the 3rd Generation Partnership Project (3GPP) in [1, Section 6.1.5]. In order to support both consistent passenger user experience and critical high-reliability train communication, the train is equipped with a relay node, which is able to distribute the communication link between all the carriages. The considered HST network is expected to support mobility of up to 500 km/h, which induces several challenges regarding physical layer design and implementation of efficient Radio Resource Management (RRM) algorithms.

High-accuracy and high-availability positioning has been considered as one of the key features in 5G networks [2], [3]. For example, as specified in [2, Table 6.3-1], regarding applications for machine control and transportation, the required positioning accuracy (in 2D), velocity estimation accuracy, and the estimation availability are given as 0.1-3 m, 0.5-2 m/s and 95%-99.9%, respectively. In this paper, we propose a novel method for HST positioning in 5G NR networks, which is able to achieve the given performance requirements. Thus, as a supplementary positioning method, the proposed approach facilitates numerous applications for railway system management from traffic control to mission-critical safety features, which have potential to boost the deployment of new 5G NR networks. In addition, as studied in [4], position information introduces a powerful asset for location-aware Radio Resource Management (RRM), including for example, location-based beamforming, mobility management and proactive resource utilization, as well as enables mitigation of signal impairments due to high-speed scenario in terms of Doppler shift compensation and transmission timing alignment.

Mobile-network-based positioning has been earlier studied, for example, in [5] regarding the fourth generation networks, and in [6], [7] regarding 5G networks. Moreover, in [8], train-side HST positioning in 5G NR has been studied based on downlink (DL) reference signals. On the contrary, in this paper the proposed positioning approach is based on network-side positioning, where the network nodes receive uplink (UL) 5G NR reference signals transmitted by the train. By this way, it is possible to provide real-time position information to the train management systems and location-aware RRM algorithms, as the position information is maintained at the network-side. By exploiting the available position information, we utilize location-based beamforming at the network nodes, and thus, avoid expensive beam training methods for searching the optimal beam directions. In order to avoid tight synchronization requirements between the train and the network, we consider Time-Difference-Of-Arrival (TDOA) for the positioning measurements. Furthermore, the train is tracked by using the

This work was partially supported by the Finnish Funding Agency for Technology and Innovation (Tekes) and Nokia Bell Labs, under the projects "Wireless for Verticals (WIVE)", "Phoenix+" and "5G Radio Systems Research", and by the Academy of Finland (under the projects 276378, 288670, and 304147).

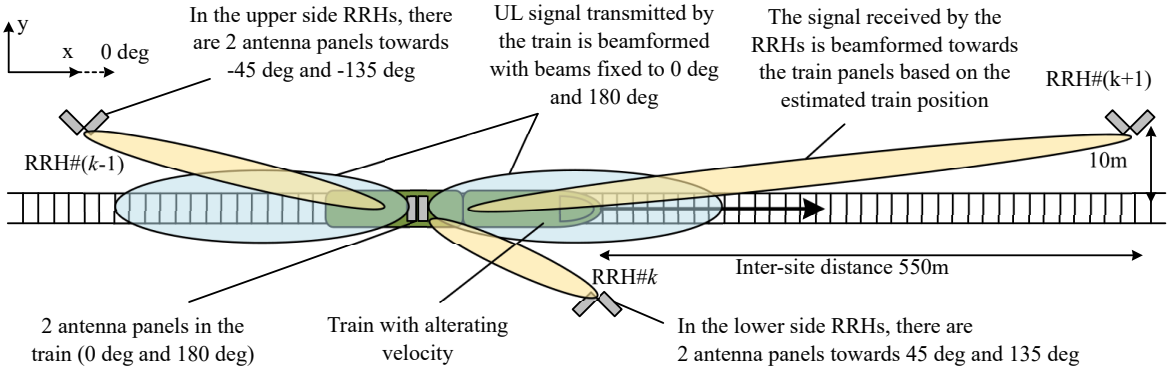

Fig. 1. Illustration of the considered HST and positioning scenario. The train transmits a periodical sounding reference signal at intervals of 100 ms with fixed TX beamformers along the track. The RX beamformers in the network RRHs are dynamically directed towards the train based on the real-time estimate of the train position.

Extended Kalman Filter (EKF), which applies linearization of the non-linear TDOA-based measurement model and provides computationally feasible approach for practical implementations. The main contributions of this paper can be described and summarized as follows:

- Efficient EKF based positioning and tracking solution, building on 5G NR uplink sounding reference signal structures and the associated TDOA measurements in the network nodes, is developed and described.
- The proposed solution and positioning concept are formulated such that setting beam directions of all network nodes is accomplished without any additional beam-training methods or reference signals.
- A novel method for selecting an optimal reference timing measurement for the TDOA, based on the Bayesian information criterion, is described.
- Efficient outlier detection methods for measurements and position estimates are developed and implemented, which are crucial for the location-based beamforming in order to avoid accumulation of positioning and beam direction error, and correspondingly losing the signal.
- Comprehensive performance evaluations complying with the 3GPP 5G NR Release'15 specifications and HST evaluation assumptions are provided, showing the availability of sub-meter positioning accuracy with at least 90% probability.

The rest of the paper is organized as follows. Section II describes the considered system model, including the HST scenario, channel models and transmit and receive signals structures. In Section III, the methods for obtaining the TDOA measurements and removing measurement outliers are developed and presented. After this, in Section IV, the considered EKF tracking algorithm is introduced. Finally, the performance of the proposed approach is evaluated and analyzed in section V, while the conclusions are drawn in Section VI.

II. System Description and Channel Model

The studied HST scenario is based on the description of the high-speed deployment model at 30 GHz carrier frequency presented in [1, Section 6.1.5]. As illustrated in Fig. 1, the network comprises Remote Radio Heads (RRH) located on alternate sides of the track at intervals of 550m. In the train, there are two antenna panels with fixed TX beams in parallel with the nose and tail of the train. The RRHs include two antenna panels facing towards both directions of the track with 45 deg rotation. However, instead of fixed beams, the RRHs utilize location-based RX beams based on the proposed positioning approach.

We assume a spatial time-varying MIMO channel, including path loss, shadowing, and fast fading effects, as specified in [9] by the 3GPP. Moreover, we assume a single layer data transmission, which is beamformed through analog/RF processing in the transmitter and receiver antenna systems by adjusting the signal phase between the antenna array elements. Thus, the m^{th} received sample at the k^{th} RRH can be written as

$$z_k[m] = \mathbf{b}_{\text{RX},k}\left(\gamma_k[m]\mathbf{\Lambda}_k[m]\mathbf{b}_{\text{TX}}u[m-\zeta_k] + \mathbf{n}_k[m]\right), \quad (1)$$

where $u[m-\zeta_k]$ is the m^{th} signal sample transmitted by the train with a fractional sample delay $\zeta_k \in \mathbb{R}_+$, defined as

$$u[m-\zeta_k] = \sum_{q=0}^{N_{\text{slot}}-1} u[q]\,\text{sinc}(m-q-\zeta_k), \quad (2)$$

where N_{slot} is the number of samples in the transmitted UL signal including a single time slot, and $\zeta_k = F_s\tau_k$ is the radio propagation delay given in fractional samples, where F_s is the sampling frequency and τ_k is the radio propagation delay for the LOS path of the k^{th} RRH. Furthermore, $\mathbf{n}_k[m] \in \mathbb{C}^{N_{\text{RX}}}$ is a vector of white Gaussian noise for each receiver antenna element, and $\mathbf{b}_{\text{TX}} \in \mathbb{C}^{N_{\text{TX}}}$ and $\mathbf{b}_{\text{RX},k} \in \mathbb{C}^{N_{\text{RX}}}$ are the steering vectors of the transmitter (i.e., the train) and the receiver (i.e., the RRH) beamformers, respectively. Moreover, $\gamma[m]_k$ is a scaling factor incorporating the effect of path loss and shadowing, based on the urban Micro (uMI) LOS scenario with the parametrization given in [9]. The spatial channel matrix $\mathbf{\Lambda}_k[m]$ models fast fading effects based on the Clustered Delay Line D (CDL-D) model with rms delay spread of 300 ns, and a spatial power delay profile as specified in [9,

Table 7.7.1-4]. In addition, $\mathbf{\Lambda}_k[m]$ incorporates the propagation delays for each cluster in relation to the propagation delay of the Line-Of-Sight (LOS) path τ_k. In order to maintain a spatial consistency between the system geometry with particular train and RRH positions and the CDL-D model with a fixed-value angle distribution, we employ the angle scaling method, specified in [9, Section 7.7.5.1].

The transmitted signal $u[m]$ consists of a single uplink (UL) time slot including 14 consecutive OFDM symbols, as defined in [10]. The positioning-related measurements in the RRHs are based on the 5G NR UL sounding reference signal (SRS) specified in [10, Section 6.4.1.4]. The SRS can be transmitted with a full band allocation or in smaller parts of the used frequency band at a time, including both aperiodic and periodic transmission configurations. However, since the SRS is mainly used for channel estimation purposes, we assume the full band SRS allocation due to the small channel coherence time in the HST scenario. Moreover, for simplicity we consider a periodic SRS transmission with 100 ms intervals, and we map the SRS symbol into the 8$^{\text{th}}$ OFDM symbol of the transmitted UL time slot.

III. Measurements and TDOA Estimation

The estimation of Time-Difference-Of-Arrival (TDOA) is based on the above-described periodic UL SRS transmitted by the train with full band resource allocation. By utilizing the TDOA, it is possible to avoid tight synchronization requirements between the train and the network, as only the network nodes are assumed to be synchronized. Furthermore, by considering the high-speed deployment model with 30 GHz carrier frequency shown in [1, Section 6.1.5], and assuming that the RRHs collecting the positioning measurements operate under the same Baseband Unit (BBU), the assumption of having synchronized clocks in the network side is reasonable. Next, in this section, we describe the proposed approach for obtaining TDOA-based ranging measurements, including propagation delay estimation, measurement validation, selection of a reference RRH for evaluating the time-differences, as well as detection of measurement outliers.

A. Estimation of Propagation Delays with a Clock Error

The positioning measurements are based on the cross-correlation between the received signal and the known SRS signal transmitted by the train. Although incorporating signal phase measurements would improve the timing measurement accuracy, we consider solely the cross-correlation approach due to its robustness and capability of operating with low SNR values. Hence, the cross-correlation function observed in the k^{th} RRH can be written as

$$r_k[l] = \sum_{m=0}^{N_{\text{slot}}-1} u^*_{\text{SRS}}[m-l]z_k[m], \tag{3}$$

where N_{slot} is the number of samples in the UL time slot, and $u_{\text{SRS}}[m]$ is the known SRS, extended with zeros in the end. Now, by simply neglecting the clock error between the train and the network, the estimate of the propagation delay for the k^{th} RRH can be obtained by finding the sample index, where the absolute value of the correlation function is maximized as

$$\hat{l}_k = \arg\max_l |r_k[l]| \text{ and } \hat{\tau}_k = \frac{\hat{l}_k}{F_{\text{s}}}, \tag{4}$$

where F_{s} is the sampling frequency, and $\hat{l}_k$ and $\hat{\tau}_k$ are the estimated propagation delay in samples and in seconds, respectively. Here, it should be emphasized that due to the clock error between the train and the network, the estimate $\hat{\tau}_k$ does not reflect the true propagation delay, but it is merely a pseudo-measurement used in the following steps of the TDOA method.

B. Measurement Validation and Estimation Error Evaluation

Due to channel fading and noise, the correlation function might be missing a clear peak and the observed maximum peak can be originated from the noise instead of the SRS. Therefore, the set of valid timing measurements, including a clear correlation peak, is determined as

$$\Omega_{\hat{\tau}} = \left\{ \hat{\tau}_k \mid \max_l\{|r_k[l]|\} > 4\sigma_{\text{corr},k} \right\} \tag{5}$$

where $\sigma_{\text{corr},k}$ is the standard deviation of the correlation function $r_k[l]$ of the k^{th} RRH.

A capability for evaluating measurement accuracies is an important feature of an accurate positioning system, as it facilitates combination of measurements from multiple RRHs with various SNR values, and enables estimation of positioning accuracy and estimation reliability. In this paper, we estimate the variance of the timing measurement $\hat{\tau}_k$ based on the estimated SNR of the received signal. As shown in [11], the maximum likelihood estimate of the SNR value for the k^{th} RRH can be obtained as

$$\hat{\xi}_k = \frac{\mathbf{z}_k^H \mathbf{\Phi} \mathbf{z}_k}{\mathbf{z}_k^H (\mathbf{I} - \mathbf{\Phi}) \mathbf{z}_k} \text{ with } \mathbf{\Phi} = \frac{\mathbf{u}_{\text{SRS}} \mathbf{u}_{\text{SRS}}^H}{N_{\text{SRS}}}, \tag{6}$$

where the vector $\mathbf{z}_k = [z_k[\hat{l}_k], z_k[\hat{l}_k + 1], \ldots, z_k[\hat{l}_k + N_{\text{SRS}} - 1]]^T$ includes the first N_{SRS} received signal samples from the beginning of the estimated correlation peak, $\mathbf{u}_{\text{SRS}} = [u_{\text{SRS}}[0], u_{\text{SRS}}[1], \ldots, u_{\text{SRS}}[N_{\text{SRS}}-1]]^T$ is the known SRS, and N_{SRS} is the length of the SRS in samples.

In order to map the estimated SNR into the timing estimate variance, we utilize the Fisher information, and define the timing estimate variance for the k^{th} RRH as

$$\hat{\sigma}^2_{\hat{\tau},k} = \frac{1}{\hat{\xi}_k B^2}, \tag{7}$$

where $\hat{\sigma}^2_{\hat{\tau},k}$ is the Cramér-Rao Lower Bound (CRLB) for the timing estimate $\hat{\tau}_k$, as given in [12], and B is the SRS bandwidth.

C. Selection of a Reference RRH with Outlier Detection

Based on the TDOA principle, the effect of the clock error between the network and the train can be eliminated

by utilizing a set of the measured time-differences between a selected reference RRH and the remaining RRHs, defined as

$$\{\hat{\tau}_k - \hat{\tau}_{k_{\mathrm{REF}}} \mid \hat{\tau}_k \in \Omega_{\hat{\tau}}, k \neq k_{\mathrm{REF}}\} \tag{8}$$

where k_{REF} is the index of the chosen reference RRH, and $\Omega_{\hat{\tau}}$ is the set of found RRH measurements, as defined in (5). Now, since the measurement of the selected reference RRH affects all time-difference measurements, it is important to select one, which provides a high-quality measurement. A straightforward solution would be selecting the reference RRH based on the highest estimated SNR. However, *the RRH measurement with the highest SNR does not necessarily originate from the LOS path*, which can result in large timing measurement errors. Therefore, in order to find the optimum reference RRH, we utilize the Bayesian Information Criterion (BIC), studied for example in [13], which exploits a priori information on the train position for selecting the reference RRH.

As described in Section IV, the train position is continuously tracked based on the Extended Kalman Filter (EKF), which enables the prediction of the train position based on the position estimates at previous time instants. Moreover, the fundamental idea of the considered BIC approach is to select a set of time-difference measurements, which fit best for the predicted train position at the given time instant. Based on this, by assuming Gaussian distributed measurement error, the log-likelihood function for the time-difference measurements between the i^{th} and j^{th} RRH can be written as

$$\begin{aligned} L_{i,j}(\Delta\tau) &= -\frac{(\Delta\tau - (\tilde{\tau}_i - \tilde{\tau}_j))^2}{2(\hat{\sigma}^2_{\hat{\tau},i} + \hat{\sigma}^2_{\hat{\tau},j})} \\ \text{with } \tilde{\tau}_l &= \frac{\|\mathbf{p}_l - \hat{\mathbf{p}}\|}{c}, \end{aligned} \tag{9}$$

where c is the speed of light, $\mathbf{p}_l \in \mathbb{R}^2$ is the known position of the l^{th} RRH, and $\hat{\mathbf{p}} \in \mathbb{R}^2$ is the predicted train position.

The validation of the timing measurements, as presented in (5), does not guarantee that the detected timing measurement is originated from a LOS path. Especially, in case of errors in directing the transmit and receive beams, it is possible that the detected measurement is originated from a NLOS path resulting in large positioning errors. Assuming Gaussian distributed measurement error, the set of RRH indices, which provides acceptable time-difference measurements for the reference RRH index k_{REF}, is given as

$$\begin{aligned} \Omega^{(k_{\mathrm{REF}})}_{\Delta\hat{\tau}} = \{k \mid\ & k \neq k_{\mathrm{REF}}, |(\hat{\tau}_k - \hat{\tau}_{k_{\mathrm{REF}}}) - (\tilde{\tau}_k - \tilde{\tau}_{k_{\mathrm{REF}}})|^2 \\ & < (\hat{\sigma}^2_{\hat{\tau},k} + \hat{\sigma}^2_{\hat{\tau},k_{\mathrm{REF}}}) \chi_2^{-1}(p_{\mathrm{L}}, 1)\} \end{aligned} \tag{10}$$

where $\chi_2^{-1}(p_{\mathrm{L}}, 1)$ is the inverse of the chi-squared distribution with 1 degree of freedom, and $p_{\mathrm{L}} \in \{p \in \mathbb{R} \mid 0 < p < 1\}$ is the probability threshold, which determines which percentage of all measurements are considered to be included in the measurement set. The measurements which fall outside the maximum allowed measurement deviation are considered as outliers. In this paper, we set $p_{\mathrm{L}} = 0.999\,(= 99.9\%)$, which helps to remove large measurement outliers originating, for example, from detecting a correlation peak of a NLOS path instead of the LOS path.

Now, based on the BIC, the index of the optimum reference RRH is estimated from the set of acceptable time-difference measurements as

$$\hat{k}_{\mathrm{REF}} = \arg\max_{k_{\mathrm{REF}}} \{ \sum_{k \in \Omega^{(k_{\mathrm{REF}})}_{\Delta\hat{\tau}}} L_{k,k_{\mathrm{REF}}}(\hat{\tau}_k - \hat{\tau}_{k_{\mathrm{REF}}}) \mid \hat{\tau}_{k_{\mathrm{REF}}} \in \Omega_{\hat{\tau}} \} \tag{11}$$

where the estimated reference RRH index $\hat{k}_{\mathrm{REF}}$ maximizes the joint likelihood of the time-difference measurements. As a result, the set of time-difference measurements, considered in the train tracking phase presented in Section IV, are given as

$$\Omega_{\Delta\hat{\tau}} = \{\hat{\tau}_k - \hat{\tau}_{\hat{k}_{\mathrm{REF}}} \mid k \in \Omega^{(\hat{k}_{\mathrm{REF}})}_{\Delta\hat{\tau}}\}. \tag{12}$$

Nevertheless, it is worth of emphasizing that in realistic positioning scenarios with channel fading and a risk of false LOS path detection, utilization of the considered outlier removal methods is extremely important. Otherwise, the considered Bayesian tracking methods might become susceptible to high errors due to inaccurately estimated measurement reliabilities.

IV. TDOA-based Train Tracking

The considered train tracking is based on the EKF [14], which linearizes the TDOA-based non-linear measurement function around the currently estimated tracking state. Compared to other tracking methods, which are able to handle non-linear measurement functions, such as particle filters, the EKF is able to provide a computationally efficient solution, which is feasible for practical implementations.

Besides the train position, also the train velocity is tracked and the state EKF state vector at the n^{th} time step is defined as

$$\mathbf{s}[n] = \left[\mathbf{p}[n]^T, \mathbf{v}[n]^T\right]^{\mathrm{T}}, \tag{13}$$

where $\mathbf{p}[n] = [x[n], y[n]]^T$ and $\mathbf{v}[n] = [v_x[n], v_y[n]]^T$ are the state of the train position and velocity with the corresponding train x-coordinate and y-coordinate, and the train velocities in the x-axis and y-axis, respectively. Furthermore, the state-transition model and the measurement model are given as

$$\begin{aligned} \mathbf{s}[n] &= \mathbf{F}\mathbf{s}[n-1] + \mathbf{q}[n] \\ \boldsymbol{\psi}[n] &= \mathbf{h}(\mathbf{s}[n]) + \mathbf{w}[n], \end{aligned} \tag{14}$$

where $\boldsymbol{\psi}[n]$ is the measurement vector, $\mathbf{F}$ is the linear state-transition matrix, $\mathbf{h}(\mathbf{s}[n])$ is the non-linear measurement function, and $\mathbf{q}[n] \sim \mathcal{N}(\mathbf{0}, \mathbf{Q})$ and $\mathbf{w}[n] \sim \mathcal{N}(\mathbf{0}, \mathbf{W})$ are the noise vectors describing the process noise and measurement noise, respectively. Moreover, $\mathbf{Q} \in \mathbb{R}^{4\times4}$ and $\mathbf{W} \in \mathbb{R}^{N_{\Delta\tau}\times N_{\Delta\tau}}$ are the covariance matrices for the process noise and the measurement noise, respectively, and $N_{\Delta\tau} = |\Omega^{(k_{\mathrm{REF}})}_{\Delta\hat{\tau}}|$ is the number of available time-difference measurements at a given time instant.

Regarding the state evolution, we consider a constant velocity model, where the train velocity is assumed to be nearly constant between two consecutive time steps. Consequently, the state-transition matrix in (14) is defined as

$$\mathbf{F} = \begin{bmatrix} \mathbf{I}_{2\times2} & \Delta t \mathbf{I}_{2\times2} \\ \mathbf{0}_{2\times2} & \mathbf{I}_{2\times2} \end{bmatrix}, \tag{15}$$

where Δt is the time interval between two consecutive states. By considering a continuous white noise acceleration (CWNA) model, as given in [15], the corresponding process noise covariance matrix is defined as

$$\mathbf{Q} = \sigma_{\mathrm{v}}^2 \begin{bmatrix} \frac{\Delta t^3}{3}\mathbf{I}_{2\times 2} & \frac{\Delta t^2}{2}\mathbf{I}_{2\times 2} \\ \frac{\Delta t^2}{2}\mathbf{I}_{2\times 2} & \Delta t\mathbf{I}_{2\times 2} \end{bmatrix}, \tag{16}$$

where σ_{v}^2 is the variance of the train velocity.

At each time step n, the EKF estimation process consists of two separate phases, the prediction phase and the update phase. In the prediction phase, the a priori estimate of the state $\hat{\mathbf{s}}^-[n]$ and the covariance $\hat{\mathbf{P}}^-[n] \in \mathbb{R}^{4\times 4}$ are obtained based on the state-transition model, given in (14), by considering the previous state a posteriori estimates $\hat{\mathbf{s}}^+[n-1]$ and $\hat{\mathbf{P}}^+[n] \in \mathbb{R}^{4\times 4}$ as

$$\begin{aligned} \hat{\mathbf{s}}^-[n] &= \mathbf{F}\hat{\mathbf{s}}^+[n-1] \\ \hat{\mathbf{P}}^-[n] &= \mathbf{F}\hat{\mathbf{P}}^+[n-1]\mathbf{F}^{\mathrm{T}} + \mathbf{Q}. \end{aligned} \tag{17}$$

After the prediction step, if there are measurements available, the a priori estimate is updated based on the non-linear measurement model shown in (14). Now, based on the obtained time-difference measurements, the measurement vector at the n^{th} time instant can be written as $\boldsymbol{\psi}[n] = [\psi_0[n], ..., \psi_{N_{\Delta\tau}-1}[n]]^{\mathrm{T}}$, where the vector elements $\psi_i[n]$ consist of the set of obtained time-difference measurements $\Omega_{\Delta\hat{\tau}}$, defined in (12). Thus, the non-linear measurement function, given in (14), can be described as

$$\begin{aligned} \mathbf{h}(\mathbf{s}[n]) &= [h_0(\mathbf{s}[n]), ..., h_{N_{\Delta\tau}-1}(\mathbf{s}[n])]^{\mathrm{T}} \text{ with} \\ h_i(\mathbf{s}[n]) &= \frac{\|\hat{\mathbf{p}}[n] - \mathbf{p}_{\mathrm{RRH},i}\| - \|\hat{\mathbf{p}}[n] - \mathbf{p}_{\mathrm{RRH},\hat{k}_{\mathrm{REF}}}\|}{c}, \end{aligned} \tag{18}$$

where $\hat{\mathbf{p}}[n]$ is the estimated train position based on the a priori state estimate $\hat{\mathbf{s}}^-[n]$, $\mathbf{p}_{\mathrm{RRH},\hat{k}_{\mathrm{REF}}}$ is the position of the reference RRH, and $\mathbf{p}_{\mathrm{RRH},i}$ is the position of the RRH, which corresponds to the i^{th} time-difference measurement in $\boldsymbol{\psi}[n]$. Furthermore, the a posteriori estimates of the update phase can be obtained as

$$\begin{aligned} \hat{\mathbf{s}}^+[n] &= \hat{\mathbf{s}}^-[n] + \mathbf{K}[n]\left(\boldsymbol{\psi}[n] - \mathbf{h}(\hat{\mathbf{s}}^-[n])\right) \\ \hat{\mathbf{P}}^+[n] &= \left(\mathbf{I} - \mathbf{K}[n]\mathbf{H}[n]\right)\hat{\mathbf{P}}^-[n], \text{ where} \end{aligned} \tag{19}$$

$$\mathbf{K}[n] = \hat{\mathbf{P}}^-[n]\mathbf{H}[n]^{\mathrm{T}}\left(\mathbf{H}[n]\hat{\mathbf{P}}^-[n]\mathbf{H}[n]^{\mathrm{T}} + \mathbf{W}\right)^{-1} \tag{20}$$

In above, $\mathbf{K}[n]$ is the Kalman gain, and $\mathbf{H}[n] \in \mathbb{R}^{N_{\Delta\tau}\times 4}$ is the Jacobian matrix of the measurement function $\mathbf{h}(\cdot)$ evaluated at $\hat{\mathbf{s}}^-[n]$, given as

$$\mathbf{H}[n] = \begin{bmatrix} \eta_0^{(x)} - \eta_{\hat{k}_{\mathrm{REF}}}^{(x)} & \eta_0^{(y)} - \eta_{\hat{k}_{\mathrm{REF}}}^{(y)} & \mathbf{0}_{1\times 2} \\ \vdots & \vdots & \vdots \\ \eta_{N_{\Delta\tau}-1}^{(x)} - \eta_{\hat{k}_{\mathrm{REF}}}^{(x)} & \eta_{N_{\Delta\tau}-1}^{(y)} - \eta_{\hat{k}_{\mathrm{REF}}}^{(y)} & \mathbf{0}_{1\times 2} \end{bmatrix} \tag{21}$$

with

$$\eta_i^{(x)} = \frac{\Delta\hat{x}_i[n]}{c\|\hat{\mathbf{p}}[n] - \mathbf{p}_{\mathrm{RRH},i}\|} \text{ and } \eta_i^{(y)} = \frac{\Delta\hat{y}_i[n]}{c\|\hat{\mathbf{p}}[n] - \mathbf{p}_{\mathrm{RRH},i}\|},$$

where $\Delta\hat{x}_i[n] = \hat{x}[n] - x_{\mathrm{RRH},i}$ and $\Delta\hat{y}_i[n] = \hat{y}[n] - y_{\mathrm{RRH},i}$ define the difference for the x and y coordinates between the estimated a priori position of the train and the i^{th} RRH, respectively. Moreover, as given in [16], the measurement covariance matrix for the obtained time-difference measurements $\boldsymbol{\psi}[n]$ is defined as

$$\mathbf{W} = \hat{\sigma}_{\hat{\tau},k_{\mathrm{REF}}}^2 + \mathrm{diag}\left(\hat{\sigma}_{\hat{\tau},0}^2, \hat{\sigma}_{\hat{\tau},1}^2, \ldots, \hat{\sigma}_{\hat{\tau},N_{\Delta\tau}-1}^2\right), \tag{22}$$

where $\hat{\sigma}_{\hat{\tau},i}^2$ is the estimate of the timing measurement variance for the RRH, which corresponds to the i^{th} measurement in $\boldsymbol{\psi}[n]$, as defined in (7).

With a *low number of available measurements, and with a specific TDOA measurement geometry, the update phase of the EKF might result in rapid changes in the estimated state vector*. In the considered location-based beamforming approach, this might lead to a fast accumulation of the positioning error, and thus, cause missing the correct beamforming direction and losing the signal. For this reason, the state vector update, presented in (19), is performed only, if

$$\begin{aligned} (\hat{\mathbf{s}}^+[n] - \hat{\mathbf{s}}^-[n])^T \hat{\mathbf{P}}^-[n]^{-1} (\hat{\mathbf{s}}^+[n] - \hat{\mathbf{s}}^-[n]) \\ < \chi_2^{-1}(p_{\mathrm{EKF}}, 2), \end{aligned} \tag{23}$$

where $\chi_2^{-1}(p_{\mathrm{EKF}}, 2)$ is the inverse of the chi-squared distribution with 2 degrees of freedom, and $p_{\mathrm{EKF}} \in \{p \in \mathbb{R} \mid 0 < p < 1\}$ is the probability, which defines the threshold for the outlier detection by rejecting unlikely state updates. If the condition in (23) is not satisfied, the state vector update is simply neglected. In this paper, we set $p_{\mathrm{EKF}} = 99.9\%$, which is considered to be high enough in order to remove only the most significant measurement outliers. This approach is shown, through simulations in the next section, to perform highly reliably.

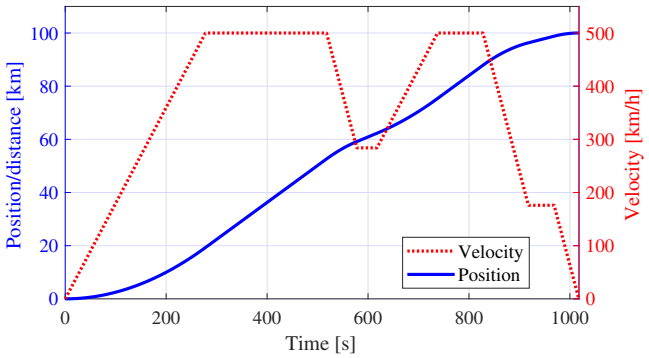

Fig. 2. The position (traveled distance) and the velocity of the train, as functions of time, assumed in the simulated HST scenario.

V. Performance Evaluation and Analysis

The performance of the proposed positioning and beamforming approach is evaluated by simulating a 100 km long rail track with RRHs located along the track, as shown in Fig. 1. By following the HST scenario specified by 3GPP in [1, Section 6.1.5], the track is defined as a straight line, which is a reasonable assumption, as the track curvature is very limited due to support for high velocities. Moreover, we assume that only the 5 closest RRHs perform timing measurements at a

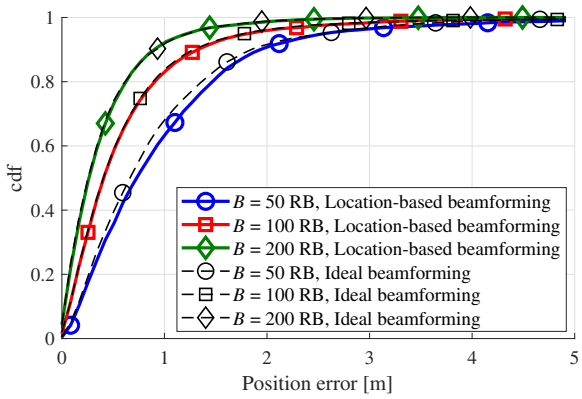

Fig. 3. Cumulative distributions of positioning errors for different bandwidth configurations, and for location-based beamforming and ideal (reference) beamforming.

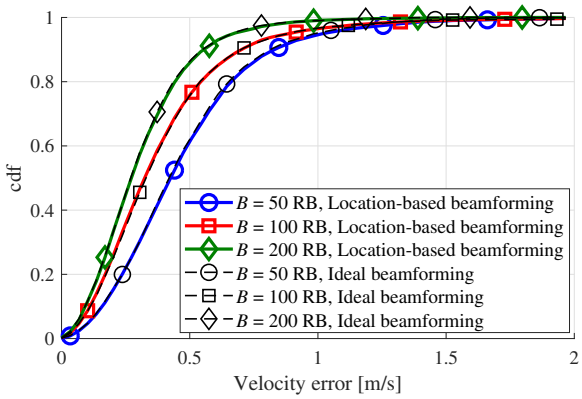

Fig. 4. Cumulative distributions of velocity estimation errors for different bandwidth configurations, and for location-based beamforming and ideal (reference) beamforming.

time, and thus, in the proximity of the active RRHs, a track with a limited curvature appears approximately as a straight line. In the beginning of the simulation, the train is still and begins to accelerate (0.5 $\mathrm{m/s^2}$) towards the top speed (500 km/h). After traveling with the top speed for 4 minutes, the train slows down (1.0 $\mathrm{m/s^2}$), but re-accelerates again, until stopping in the end. The position and velocity of the train during the considered simulation path and time are shown in Fig. 2.

The positioning is based on the UL SRS, which is mapped into the eighth OFDM symbol transmitted at 100 ms intervals. The other OFDM symbols inside the time slot comprise random QPSK-modulated subcarriers. By considering the HST scenario with high velocity and 30 GHz carrier frequency, and thus a wide Doppler spread, the subcarrier spacing is set to 120 kHz. However, based on our preliminary studies, also other subcarrier spacing values are feasible with the considered positioning approach. On the other hand, when considering communications signals with tight requirements for tolerable inter-carrier interference levels, reduced subcarrier spacing might limit the system performance. The carrier frequency and the UL transmit power are defined as 30 GHz and 33 dBm, respectively. The considered channel model, including the path loss, shadowing and fast fading, is as described in Section II. Furthemore, the noise spectral density and the RRH noise figure are defined as -174 dBm/Hz and 5 dB, respectively,

The number of antenna elements in a single antenna panel is given as $N_{\mathrm{RX}} = 32$ for the RRHs, and $N_{\mathrm{TX}} = 8$ for the train. Whereas at the train side the TX beams are fixed towards the nose and the tail of the train, the RX beams at the RRH side are directed towards the estimated train position at each SRS transmit time. Here, it should be emphasized that the RRH beam directions are based on the train position estimate available after the prediction step of the EKF (i.e., $\hat{\mathbf{s}}^{-}[n]$)). Only after obtaining the measurements by using the prediction-step-based RX beamformer, the a posteriori estimate (i.e., $\hat{\mathbf{s}}^{+}[n]$)) can be acquired, and further used for estimating the new beamformer parameters for the subsequent SRS transmission time. Thus, since the used RRH beam direction is always based on the prediction-step of the EKF, the maximum allowed latency for updating the position estimate is limited by the SRS transmit interval.

In Fig. 3 the cumulative distributions of the achieved position errors are shown for 3 separate bandwidth configurations, including 50 Resource Blocks (RB), 100 RBs, and 200 RBs, which correspond with physical bandwidths of 72 MHz, 144 MHz and 288 MHz, respectively. As expected, the positioning accuracy can be improved by increasing the transmission bandwidth. With the maximum considered bandwidth of 200 RBs, 1 m positioning accuracy is achieved with 90% availability, whereas with the 50 RB bandwidth, the corresponding accuracy is 2.1 m. Besides using the location-based beamforming relying on the train position estimates at the network-side, also the reference results assuming ideal beam directions are provided for comparison purposes. For most of the time, the proposed location-based beamforming approach loses only a few centimeters to the case with ideal beam directions.

The cumulative distributions of the velocity errors are shown in Fig. 4 for the considered bandwidths. Similar to the positioning accuracy, the velocity accuracy is improved by increasing the bandwidth. With the highest considered bandwidth of 200 RBs, velocity error below 1 m/s can be achieved with 97 % availability. The estimation of train velocity is very important for railway safety applications, and it can also enable, e.g., Doppler shift compensation, which can considerably increase the system throughput in the considered HST scenario.

In order to efficiently utilize the location-based beamforming for enhancing the network capacity, the accuracy of the RRH beam directions is essential. In Fig. 5 the cumulative error distributions of the beam direction are shown for the considered bandwidths. As expected, since the accuracy of the RRH beam directions are dependent on the positioning accuracy, larger bandwidths provide better beam direction accuracy. The shown beam direction errors are considered

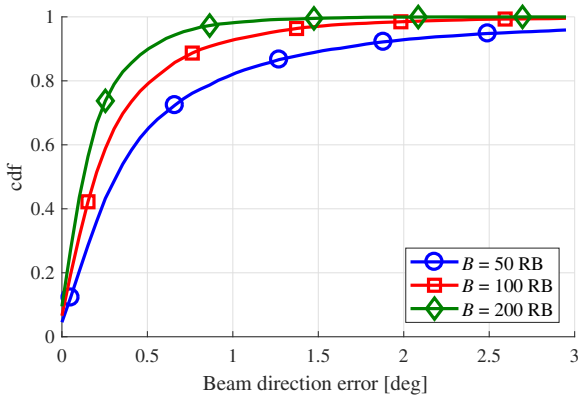

Fig. 5. Cumulative error distributions of RRH beam directions for different bandwidth configurations.

only for the closest RRH at a time, in which the beam direction accuracy is the most sensitive to positioning errors. Obviously, for a given position estimation accuracy, the beam direction error reduces as the distance to the RRH is increased. Nonetheless, the results shown in Fig. 5 indicate that a sub-degree beam direction error with 90% availability can be achieved by using the 100 RB and 200 RB bandwidths.

Considering the target accuracies for the position and velocity estimation in machine control and transportation use cases, given as 0.1-3 m and 0.5-2 m/s in [2, Table 6.3-1], the proposed approach is able to meet the performance requirements. With both the 50 RB and the 100 RB bandwidth configuration, the positioning accuracy is below 3 m with 95% availability. Furthermore, with the maximum bandwidth of 200 RBs the 3 m accuracy is achieved with 99% availability, and with 95% availability the corresponding positioning accuracy is 1.5 m. All bandwidth configurations achieve below 2 m/s velocity estimation error with 99% availability, and with the maximum considered bandwidth, 0.75 m/s estimation error is provided with 95% availability.

VI. Conclusions

In this paper, we studied network-side positioning and location-based beamforming for the HST scenario in 5G NR networks. Assuming TDOA-based positioning measurements obtained from the UL SRS transmitted by the train, we proposed a method for optimal reference measurement selection, and introduced outlier removal methods for increased system stability. We utilized a TDOA-based EKF for tracking the train position and velocity, and for providing the necessary position information for the considered network-side location-based beamforming.

Based on extensive simulation of 100 km long train track, we evaluated the train positioning performance for the 3GPP-specified 5G NR high speed scenario with location-based beamforming on the network side. The results with the highest considered bandwidth of 288 MHz show that a sub-meter positioning accuracy can be achieved with 90% availability, and below 3 m accuracy with 99% availability. Both the position and velocity estimation accuracies of the proposed approach meet the 3GPP-specified requirements regarding machine control and transportation use cases. Therefore, the revealed positioning potential of forthcoming 5G networks, can be considered as a valuable asset for future railway management systems, and is able to facilitate efficient RRM implementations, including the location-based beamforming.

References

[1] 3GPP TR 38.913 v14.3.0 Technical Specification Group Radio Access Network, Std.

[2] 3GPP TR 22.872 V2.0.0 Technical Specification Group Services and System Aspects, *Study on positioning use cases (Release 16)*, Std., May 2018.

[3] 3GPP TR 22.862 V14.1.0 Technical Specification Group Services and System Aspects, *Feasibility Study on New Services and Markets Technology Enablers for Critical Communications, Stage 1 (Release 14)*, Std., Sept. 2016.

[4] T. Levanen, J. Talvitie, R. Wichman, V. Syrjälä, M. Renfors, and M. Valkama, "Location-aware 5G communications and Doppler compensation for high-speed train networks," in *2017 European Conf. on Networks and Commun. (EuCNC)*, June 2017, pp. 1–6.

[5] C. Y. Chen and W. R. Wu, "Three-Dimensional Positioning for LTE Systems," *IEEE Trans. Veh. Technol.*, vol. 66, no. 4, pp. 3220–3234, April 2017.

[6] M. Koivisto, M. Costa, J. Werner, K. Heiska, J. Talvitie, K. Leppänen, V. Koivunen, and M. Valkama, "Joint Device Positioning and Clock Synchronization in 5G Ultra-Dense Networks," *IEEE Trans. Wireless Commun.*, vol. 16, no. 5, pp. 2866–2881, May 2017.

[7] X. Cui, T. A. Gulliver, J. Li, and H. Zhang, "Vehicle Positioning Using 5G Millimeter-Wave Systems," *IEEE Access*, vol. 4, pp. 6964–6973, 2016.

[8] J. Talvitie, T. Levanen, M. Koivisto, K. Pajukoski, M. Renfors, and M. Valkama, "Positioning of high-speed trains using 5G new radio synchronization signals," in *2018 IEEE Wireless Communications and Networking Conference (WCNC)*, April 2018, pp. 1–6.

[9] 3GPP TR 38.901 v14.3.0 Technical Specification Group Radio Access Network, *Study on channel model for frequency spectrum above 6 GHz (Release 14)*, Std., Dec. 2017.

[10] 3GPP TS 38.211 V1.0.0 Technical Specification Group Radio Access Network, *NR Physical channels and modulation (Release 15)*, Std., Sept. 2017.

[11] A. Wiesel, J. Goldberg, and H. Messer-Yaron, "SNR estimation in time-varying fading channels," *IEEE Transactions on Communications*, vol. 54, no. 5, pp. 841–848, May 2006.

[12] S. M. Kay, *Fundamentals of Statistical Signal Processing: Estimation Theory*. Prentice Hall, 1993.

[13] E. Wit, E. Van den Heuvel, and J.-W. Romeijn, "All models are wrong: An introduction to model uncertainty," vol. 66, 08 2012.

[14] D. Simon, *Optimal State Estimation: Kalman, H Infinity, and Nonlinear Approaches*. John Wiley and Sons Inc., 2006.

[15] T. K. Y. Bar-Shalom, X. R. Li, *Estimation with Applications to Tracking and Navigation: Theory, Algorithms and Software*. John Wiley and Sons, Inc., 2002.

[16] A. D. S. Sand and C. Mensing, *Positioning in Wireless Communications Systems*. John Wiley and Sons Ltd., 2014.